

Polymer Chemistry

Accepted Manuscript

This article can be cited before page numbers have been issued, to do this please use: A. Haddleton, T. M. Bennett, X. Chen, R. L. Atkinson, V. Taresco and S. M. Howdle, *Polym. Chem.*, 2020, DOI: 10.1039/D0PY00729C.



This is an Accepted Manuscript, which has been through the Royal Society of Chemistry peer review process and has been accepted for publication.

Accepted Manuscripts are published online shortly after acceptance, before technical editing, formatting and proof reading. Using this free service, authors can make their results available to the community, in citable form, before we publish the edited article. We will replace this Accepted Manuscript with the edited and formatted Advance Article as soon as it is available.

You can find more information about Accepted Manuscripts in the [Information for Authors](#).

Please note that technical editing may introduce minor changes to the text and/or graphics, which may alter content. The journal's standard [Terms & Conditions](#) and the [Ethical guidelines](#) still apply. In no event shall the Royal Society of Chemistry be held responsible for any errors or omissions in this Accepted Manuscript or any consequences arising from the use of any information it contains.

Synthesis of Two-phase Polymer Particles in Supercritical Carbon Dioxide

View Article Online
DOI: 10.1039/D0PY00729C

Alice J. Haddleton,^a Thomas M. Bennett,^a Xinyong Chen,^b Rachel L. Atkinson,^a Vincenzo Taresco^a, and Steven M. Howdle.*^a

^a School of Chemistry, University of Nottingham, Nottingham, NG7 2RD, UK.

^b School of Pharmacy, University of Nottingham, Nottingham, NG7 2RD, UK

Abstract

The synthesis of particles with discrete phases using traditional emulsion polymerisation is a well-established process. Phase-separated particles have a wide range of applications, such as in coatings, drug delivery, impact modification and as supports in catalysis. However, as a dry powder is often desired for the end application, post-polymerisation, energy intensive drying steps are usually required for the removal of water. Alternatively, dispersion polymerisation utilising supercritical carbon dioxide (scCO₂) as a reaction medium allows for the production of dry, free-flowing powders upon release of the CO₂. Here, we present the innovative use of scCO₂ to provide a novel and environmentally acceptable route for creating phase-separated particles. Particles containing a high T_g poly(methyl methacrylate) (PMMA) phase, combined with a low T_g polymer phase of either poly(benzyl acrylate) (PBzA) or poly(butyl acrylate) (PBA), were investigated. Both monomers were added to the reaction after the formation of PMMA seed particles. Benzyl acrylate (BzA) was chosen as a model low T_g monomer, with well-defined and detectable functionality when mixed with PMMA. Butyl acrylate (BA) was also used as an alternative, more industrially relevant monomer. The loading of the low T_g monomer was varied and full characterisation of the particles produced was performed to elucidate their internal morphologies and compositions.



Introduction

View Article Online
DOI: 10.1039/D0PY00729C

Supercritical carbon dioxide (scCO₂) is a sustainable reaction medium for polymerisations and is a promising alternative to conventional solvents. This is because of its tuneable properties, high natural abundance and easily accessible critical point; $T_c = 31.1\text{ }^\circ\text{C}$ and $p_c = 73.8\text{ bar}$.^{1,2} CO₂ is also inexpensive, non-toxic, non-flammable and is readily available in high purity. These properties, coupled with the fact that scCO₂ reverts to its gaseous state upon depressurisation, eliminating energy intensive drying steps, make it a desirable solvent for polymerisations.³ In 1992, DeSimone et al. published the first polymerisation utilising scCO₂ as a reaction medium, reporting the synthesis of fluoropolymers.⁴ Since then, many different polymerisations including free radical chain growth, cationic chain growth, oxidative coupling, transition metal catalysis and melt phase condensation have been carried out employing scCO₂ as the solvent, with vinyl monomers predominantly being used.^{3,5-10}

More specifically, scCO₂ has been shown to be a versatile medium for dispersion polymerisation, facilitated by the use of amphiphilic surfactants including fluoro-polymers and polysiloxanes, which are soluble in scCO₂.¹¹ Recently, increasingly more sophisticated chemistries have been reported using scCO₂ as a reaction medium. The three most widely used reversible-deactivation radical polymerisation (RDRP) techniques; nitroxide-mediated radical polymerisation (NMP), atom transfer radical polymerisation (ATRP) and reversible addition-fragmentation chain transfer polymerisation (RAFT), have all been used to synthesise well-defined particles with narrow size distributions.¹²⁻¹⁶ These techniques can give access to more complex structures including cross-linking,¹⁷ metal nanoparticles,¹⁸ and more recently block copolymer particles with internal phase separation.¹⁹⁻²¹

Particles with phase-separated internal morphologies are usually synthesised via emulsion-based techniques, typically with size between 60 - 700 nm.^{22,23} Many different internal



morphologies have been achieved using emulsion polymerisation, including core-shell. The changes in internal morphology observed occur by variation of several different parameters, such as manipulation of particle size, monomer ratio and tuning of the reaction medium.^{24,25} However, the products are obtained in the form of a latex and energy intensive steps (e.g. spray drying) are needed for the removal of water, to afford a dry powder.²⁶ Dispersion polymerisation in scCO₂ produces dry, free flowing powders upon release of the CO₂ post polymerisation. Employing dispersion polymerisation also allows for synthesis of particles between 0.5 - 5 μm, relatively large in comparison to those produced by emulsion polymerisation.²⁷ Although there is an energy cost associated with the compression of the CO₂ used in the supercritical reactions, this is an order of magnitude lower than the cost associated with the removal of water.²⁸

There are several examples of copolymer particles, synthesised in scCO₂, which exhibit micro-phase separation to give various internal particle morphologies.^{19-21,29} Cao et al. described the preparation of graft copolymer nanoparticles in scCO₂ from a one-step polymerisation. Particles of thermo-responsive poly(N-isopropylacrylamide) (PNIPAM) were synthesised with the assistance of a synthetic, graft copolymer surfactant consisting of pH-sensitive, poly(dimethylsiloxane)-*graft*-polyacrylates (PDMS-*g*-PAA). The polymers obtained were fine, free-flowing powders with monodispersed nano-sized particles being formed. The structure was confirmed as a PNIPAM core coated in a PDMS-*g*-PAA shell by TEM.³⁰

When using homopolymers rather than copolymers, a core-shell structure is typically achieved, in which one polymer phase is encased in another. Core-shell polymeric particles are desirable for a wide range of applications such as drug delivery,³¹ electrophoretic displays,³² and as impact modifiers.³³



McAllister et al. reported the synthesis of core-shell particles consisting of poly(2-(dimethylamino) ethyl methacrylate) (PDMAEMA) and PMMA via a multi-stage dispersion polymerisation.³² PMMA particles were modified in scCO_2 to give a core-shell morphology with domains of PDMAEMA within PMMA. By contrast, particles synthesised in traditional solvents produced the inverse of this, with a core of PMMA surrounded by a shell of PDMAEMA. The observed difference in structure was attributed to the ability of scCO_2 to plasticise the PMMA, allowing the DMAEMA monomer, and therefore the growing polymer, to penetrate the particles. This plasticisation does not readily occur in traditional solvents and hence, the PDMAEMA remains at the surface of the particles.

Here, we report the synthesis of particles containing both a polymer phase with a low glass transition temperature (T_g); either poly(butyl acrylate) (PBA) or poly(benzyl acrylate) (PBzA), combined with a high T_g poly(methyl methacrylate) (PMMA) phase. Both PBzA and PBA exhibit relatively low T_g s of 2 °C and -45 °C respectively, as measured by DMA, in comparison to PMMA (144 °C). This value is higher than the T_g of PMMA measured by DSC, often reported in literature as 105 °C.^{34,35} However, differences between the values obtained from the two analytical techniques do occur because of the intrinsic difference between the static DSC and the dynamic DMA measurement, resulting in the DSC observed T_g s being lower in absolute values.³⁶ The particles were formed by incorporation of the low T_g monomers to preformed PMMA particles via a simple two-step free radical polymerisation. BzA was chosen as a model low T_g monomer, with well-defined and detectable functionality when mixed with PMMA. Notably, the PBzA phase can be selectively stained prior to TEM analysis due to the presence of the aromatic group. BA as an alternative low T_g monomer was also investigated, as it is more traditionally used in commercial polymers. In both systems, the low T_g monomer loading was varied and a series of analytical techniques were used to probe and confirm the



morphologies and compositions of the particles produced. Particles that combine both low and high T_g polymer phases can be used as impact modifiers.^{37,38}

View Article Online
DOI: 10.1039/C9PY00729C

Experimental

Materials

Methyl methacrylate (MMA, ProSciTech, 99%), 2,2'-Azobis(isobutyronitrile), benzyl acrylate (BzA, Alfa Aesar, 98%), butyl acrylate (BA, BASF), (AIBN, Sigma Aldrich, 98%), and methacrylate terminated polydimethylsiloxane (PDMS-MA, 150-200 cP, ABCR GmbH & Co.) were all used as received. All reactions were carried out in SCF grade 4.0 CO₂ (≥99.99 %, BOC special gases).

Polymer Synthesis in 60 mL Autoclave

All reactions were performed in a 60 mL high-pressure autoclave built in-house, previously used for dispersion polymerisations.^{12,19,39} These experiments can also be performed at a larger scale (1 L).⁴⁰

PMMA/PBzA Particles Synthesis

MMA (Table 1) was deoxygenated by purging with argon for 30 minutes. A mixture of AIBN (1 wt% with respect to (wrt) total monomer, 0.0705 g, 0.43 mmol) and PDMS-MA (5 wt% wrt total monomer, 0.3525 g, 0.04 mmol) was separately flushed with argon for 30 minutes.

Table 1: Amount of MMA and BzA used for each loading. Loading wt% wrt total monomer.

Entry	MMA (mL)	MMA (mmol)	BzA Target Loading (wt%)	BzA (mL)	BzA (mmol)
1	9	84	9	0.79	5.16
2	8.1	75	27	1.58	10.34
3	7.2	67	36	3.16	20.65



The autoclave was deoxygenated by purging with CO₂ for 30 minutes at 1-2 bar. The MMA was combined with the AIBN/PDMS-MA and injected into the autoclave via a syringe under a positive pressure of CO₂. The autoclave was sealed, pressurised at 48 bar, and heated to 65 °C before the addition of further CO₂ to reach the desired reaction pressure (207 bar). The beginning of the reaction was recorded as the moment at which the temperature reached 65 °C, an appropriate temperature for the initiating species, after which the reaction was left stirring (300 rpm) for 4 hours. Subsequently, a charge of BzA (Table 1) was added via a high-performance liquid chromatography (HPLC) pump (0.2 mL min⁻¹), inducing a small pressure increase. The reaction was left overnight (18 hours). After this time, the heating jacket was removed, and the autoclave was allowed to naturally cool to room temperature before being depressurised. The resulting products were typically collected from the base of the autoclave as free-flowing white powders (Figure 1, stages 1, 2 & vent).

As the BzA feed was increased to deliver a loading of 50 wt%, the quality of the particles produced using a one-stage addition of BzA was reduced, with SEM analysis showing high levels of aggregation (Figure SI-1). In an attempt to improve this, the BzA was added over two-stages, as this had previously been reported to reduce agglomeration.²⁷ The initial stage of the reaction remained the same as described above. The total amount of monomer was increased to 12 mL to allow for sufficient amounts of MMA needed for nucleation in the primary loading (6.38 mL, 59.3 mmol). The PDMS-MA concentration was kept constant (5 wt% wrt total monomer, 0.6 g, 0.06 mmol), as was the AIBN concentration (1 wt% wrt total monomer, 0.12 g, 0.73 mmol). After 4 hours, the first charge of BzA (2.83 mL, 18.5 mmol) was added via an HPLC pump (0.2 mL min⁻¹), which induced a small pressure increase. The reaction was left overnight (18 hours). Subsequently, a second charge of BzA (2.83 mL, 18.5 mmol) was added via an HPLC pump (0.2 mL min⁻¹). The half-life for AIBN under these reaction conditions



is 24 hours.⁴¹ As the reaction had been carried out for approximately 24 hours at this point, additional AIBN (0.059 g, 0.33 mmol) was included in the second charge of BzA. As before, the injection induced a small pressure increase. The reaction was left overnight (18 hours), before being cooled to room temperature and depressurised. The resulting products were typically collected from the base of the autoclave as free-flowing white powders (Figure 1).

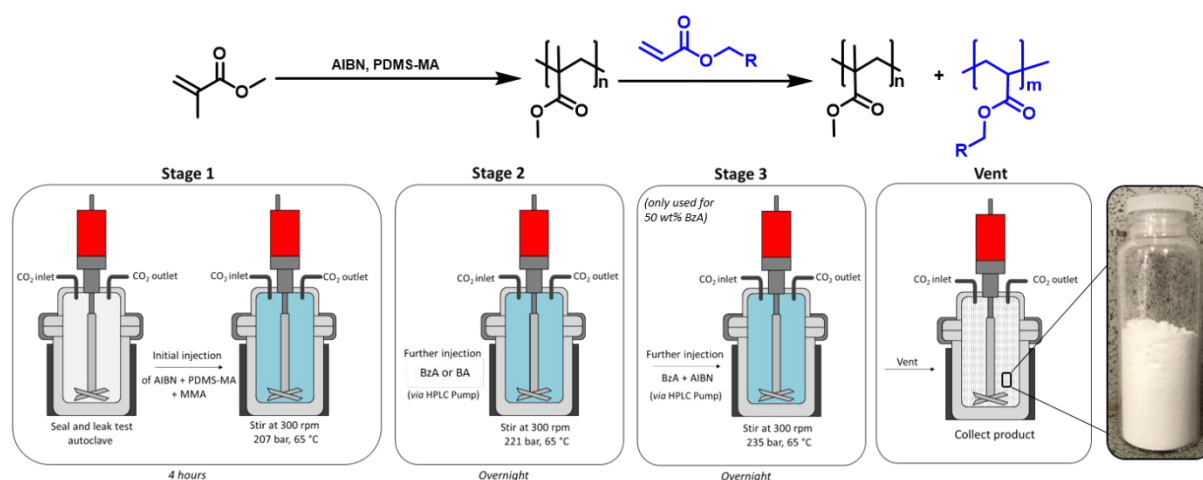


Figure 1: Schematic representation of the reaction procedure used for particle synthesis. Stage 1: synthesis of PMMA seed particles, stage 2: addition of second monomer and stage 3: for higher loadings of BzA (50 wt%) addition of the second monomer was split over two aliquots to maintain particle structure. Post venting of the reactor, free-flowing white powders were obtained.

PMMA/PBA Particles Synthesis

MMA (Table 2) was deoxygenated under argon for 30 minutes. A mixture of AIBN (1 wt% wrt total monomer, 0.0705 g, 0.43 mmol) and PDMS-MA (5 wt% wrt total monomer, 0.3525 g, 0.04 mmol) was separately flushed with argon for 30 minutes. The same process as described for the PMMA/PBzA particles synthesis above was used, with the addition of BzA substituted for BA (Table 2). The resulting products were typically collected from the base of the autoclave as free-flowing white powders (Figure 1, stages 1, 2 & vent).



Table 2: Amount of MMA and BA used for each loading. Loading wt% wrt total amount of monomerView Article Online
DOI: 10.1039/D0PY00729C

Entry	MMA (mL)	MMA (mmol)	BA Target Loading (wt%)	BA (mL)	BA (mmol)
1	9.0	84	9	0.94	6.53
2	7.2	67	27	2.82	19.58

Polymer Characterisation

Details of the homopolymers synthesised for analytical comparison are given in the supporting information (SI).

Scanning Electron Microscopy

Scanning Electron Microscopy (SEM) was performed on a Phillips XL30 microscope. Particles were washed by centrifuging in dodecane three times (10 minutes, 4000 rpm) to remove residual stabiliser, before being dispersed in dodecane onto a glass slide and dried prior to coating in platinum. Particle size was calculated from SEM images as the average diameter of 100 particles.

Size Exclusion Chromatography

Size exclusion chromatography (SEC) was performed in THF (HPLC grade, Fisher Scientific) as the eluent at room temperature, using two Agilent PL-gel mixed-D columns in series with a flow rate of 1 mL min⁻¹. A multi-angle light scattering (MALS, Wyatt Optilab Dawn 8+) detector, along with a differential refractometer (DRI, Agilent 1260), were used for sample detection. The system was calibrated using PMMA standards (molecular weight range: 1,000 - 400,000 g mol⁻¹).



Dynamic Mechanical Analysis

Measurements were performed on a Triton Technologies (now Mettler Toledo DMA1) dynamic mechanical analyser (DMA) using the powder pocket accessory. The use of this attachment allowed for direct measurement of the synthesised powder with no further sample preparation required. The sample ($40 \text{ mg} \pm 5 \text{ mg}$) was weighed into a powder pocket. Samples were measured at 1 and 10 Hz in single cantilever bending geometry between 25 to 250 °C or -100 to 250 °C depending on the region of interest. The T_g was recorded as the peak temperature of the $\tan \delta$ trace obtained at 1 Hz.

Transmission Electron Microscopy

Transmission electron microscopy (TEM) was used to analyse the internal morphology of the particles. The analysis was performed using a FEI Technai Bio Twin-12 electron microscope with an accelerating voltage of 2.2 kV. Prior to imaging, the samples were set in an epoxy resin. The resin consisted of Agar 100 resin, dodeceny succinic anhydride (DDSA), methyl nadic anhydride (MNA) and benzyl dimethyl amine (BDMA) in the ratios 2.5: 4.5: 6.0: 0.6 by volume. The resin was sectioned using an RMC Powertome XL ultramicrotome and a diamond knife. The resulting sections (<100 nm thick) were placed on a copper TEM grid. The grids were stained for 4.5 hours with RuCl_4 , which was made *in situ* by combining 12.4 mg of RuCl_3 with a solution of 4.2 mg NaIO_4 in 1 mL H_2O .

Nuclear Magnetic Resonance

The conversion and polymer content of each reaction was determined using ^1H nuclear magnetic resonance (^1H NMR) spectroscopy. Samples were dissolved in CDCl_3 and analysed using a Bruker DPX 400 MHz spectrometer. For reactions containing PBZA, analysis was performed in acetone- d_6 and tetramethylsilane (TMS) was used as a reference.



Atomic Force Microscopy

View Article Online
DOI: 10.1039/D0PY00729C

Atomic force microscopy (AFM) allowed for probing of the surface of the synthesised polymer particles. Particles were washed by centrifuging in dodecane three times (10 minutes, 4000 rpm) to remove residual stabiliser before being dispersed in dodecane onto a glass slide and dried prior to analysis. Measurements were conducted on a Dimension FastScan AFM (Bruker Corporation), working in PeakForce quantitative nanomechanical property (PF-QNM) mode in air with an RTESPA-150 silicon probe (spring constant = 2.44 N m⁻¹).

Results and Discussion

In order to synthesise phase-separated particles containing both hard and soft domains in scCO₂, the hard polymer must be synthesised first. It is known that the dispersion polymerisation of low T_g monomers in scCO₂ does not readily produce particles. The main reason for this is the fact that the CO₂ readily plasticises the polymer particles, lowering their T_g and causing agglomeration.^{42,43} For this reason, dispersion polymerisation of the higher T_g MMA was performed first, to create a stable seed particle. The second low T_g monomer was subsequently added using methodologies that have previously been reported in the literature.^{27,32,42,44,45} The initial focus of this research was the synthesis of particles containing a PBzA phase (Table 3), as a model system.

Table 3: Summary of two-stage reactions carried out with various loadings of BzA. All reactions were completed in duplicate to check batch-to-batch variability.

Entry	BzA Target Loading (wt%)	PBzA Content ^a (wt%)	BzA Conversion ^a (%)	BzA Loading by NMR ^{a*} (wt%)	Particle Size ^b (nm)
1	0	0	0	0	1640 ± 220
2	9	8	100	10	1470 ± 245
3	27	29	97	29	1140 ± 230
4	36	35	97	36	1125 ± 220
5	50	46	99	46	960 ± 220

^a - calculated from ¹H NMR, ^b - measured from SEM images (including standard deviation), *calculated post reaction from unreacted BA and PBA content.



The conversion of BzA was calculated from the ^1H NMR spectrum by comparing the integral of the unreacted vinyl peak in the monomer (Figure 2, $\delta = 6.20$ ppm, c) to the polymer peak (Figure 2, $\delta = 5.00$ ppm, d'). Unreacted BzA (Figure 2, $\delta = a, b$ and c) could affect the T_g but, if necessary, could be removed by flushing with CO_2 post reaction. This was not necessary here as very little monomer remained. The PBzA content was calculated from ^1H NMR by comparing the integral of the PMMA peak (Figure 2, $\delta = 3.63$ ppm, f') to the PBzA peak (Figure 2, $\delta = 5.00$ ppm, d'). The PBzA content of the particles was similar to the feed for all loadings of BzA. This was expected, because of the high conversion of BzA (>97%) (Table 3). The loading of BzA measured post reaction by ^1H NMR (unreacted monomer + polymer) was similar to the target loading (Table 3).

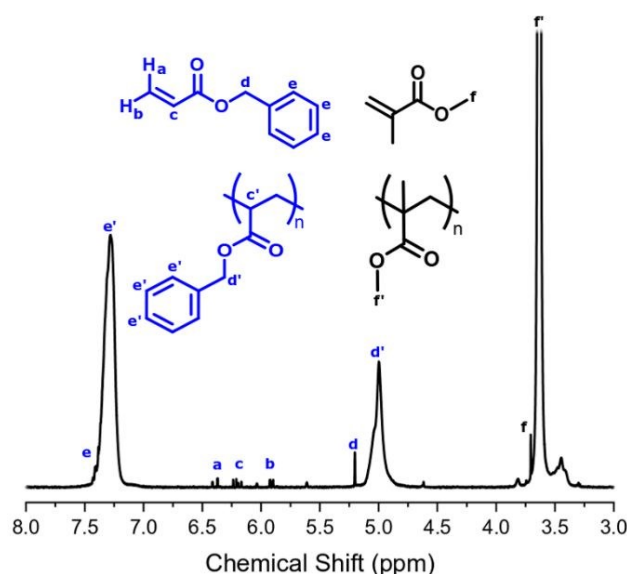


Figure 2: ^1H NMR spectrum for a reaction product containing PBzA, referenced against TMS (run in acetone). Integration values were used to calculate conversion and content of the second monomer. The depicted NMR is from a reaction carried out using a BzA loading of 27 wt%, employing the two-stage experimental method.

Surprisingly the NMR spectrum also contained trace levels of unreacted MMA, even after the long reaction time (> 48 hours). A possible explanation for this could be that the remaining



MMA is trapped in a different phase (continuous phase or polymer phase) to the propagating radicals and hence is unable to polymerise.

It should be noted that the observed decrease in particle size, as the soft component increased, is a result of variations in the amount of PDMS-MA stabiliser used (Table 3). This is because the total amount of monomer in the reaction is constant, therefore as the loading of BzA is increased, the amount of MMA in the initial stage of the reaction is reduced. However, the amount of PDMS-MA remains the same (wrt total amount of monomer). Therefore, the ratio of PDMS-MA to MMA increases. It is well known that in dispersion polymerisation the ratio of surfactant (PDMS-MA) to monomer (MMA) dictates the size of the particles produced, with higher levels of surfactant producing smaller particles.⁴⁶

GPC analysis offered significant insight into the polymer species that were present (Figure 3). At least two peaks were detected in the GPC chromatograms for all loadings of BzA. PBzA is UV active at 260 nm, whereas PMMA is not (Figure SI-2). Overlays of the UV and DRI signals, from the GPC, for all loadings of BzA indicated the presence of a UV active species (Figure 3), which in all cases is the high molecular weight species. At the point at which the second monomer is introduced, the concentration of AIBN is low and it is expected that any new polymer formed will be high molecular weight PBzA homopolymer. A further possible explanation for the higher molecular weight PBzA could be the presence of branching, that is sometimes observed with free radical polymerisation of acrylates.⁴⁷ A GPC chromatogram of pure PMMA particles is shown in the SI (Figure SI-3).



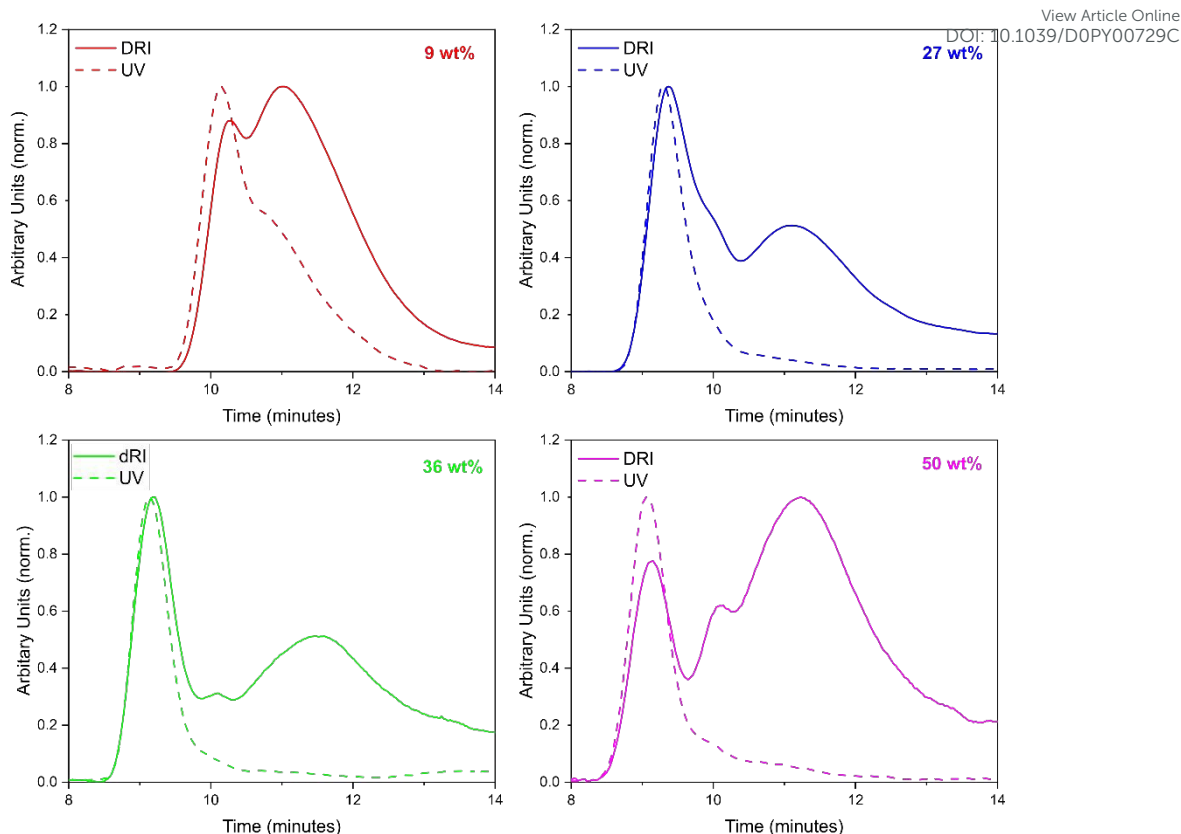


Figure 3: GPC traces obtained for sample synthesised with a 9 wt% (red), a 27 wt% (blue), 36 wt% (green) and 50 wt% (pink) BzA feed. The DRI signals are shown as a solid line and the UV signals, recorded on the samples containing PBzA, are shown as a dashed line. The DRI traces indicate the presence of two species and the UV traces indicate that one of these species is PBzA for all loadings.

Dynamic mechanical analysis (DMA) was used to establish whether phase separation has occurred within the particles. Measurements were performed using the powder pocket accessory. The use of this attachment allowed for direct measurement of the synthesised powder with no further sample preparation required. It is well known that hard-soft, core-shell particles show two $\tan \delta$ peaks, with the lower temperature peak corresponding to the soft-rubbery phase and the higher temperature peak corresponding to the hard-glassy phase.⁴⁸ For comparison, DMA data recorded for pure PMMA particles and for pure PBzA are shown in black and grey respectively (Figure 4). The DMA trace for pure PMMA particles shows one clear peak, at 144 °C, corresponding to the DMA measured T_g of the PMMA phase (Figure 4, black traces).



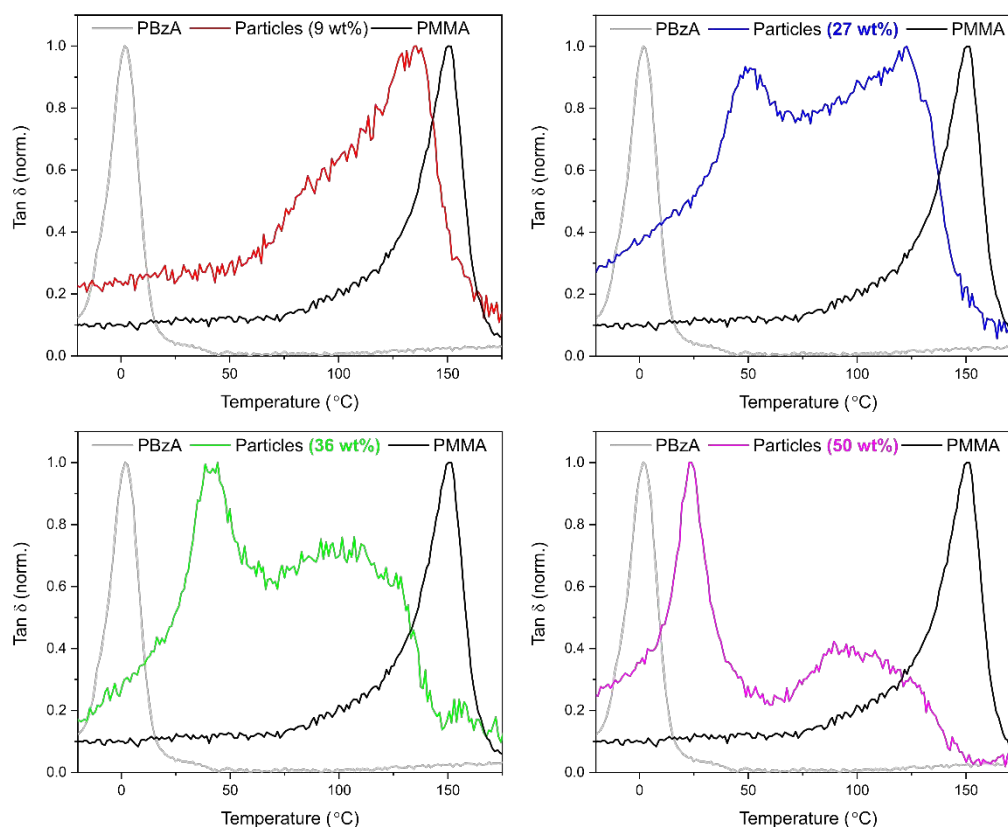


Figure 4: DMA traces for PMMA samples synthesised with a feed of BzA; 9 wt% (red), 27 wt% (blue), 26 wt% (green) and 50 wt% (pink). A homopolymer of PBzA (grey) and PMMA particles (black) is shown for comparison. Only one transition was observed for a loading of 9 wt% in comparison to the two seen for higher loadings.

For the particles produced using a 9 wt% loading of BzA, one transition was observed (Figure 4, red trace, 133 °C), similar to the peak observed for pure PMMA (144 °C), suggesting phase separation had not occurred. The small reduction in T_g in comparison to PMMA suggests that some blending of the two polymers has occurred. By contrast, as the loading of BzA was increased, a second lower T_g peak becomes visible and is attributed to a PBzA rich phase, whereas the high T_g peak is attributed to a PMMA rich phase.

A shift in T_g from the pure polymers was observed, suggesting that the phases present are not 100% separated but partially blended. However, as the loading of the BzA increases, the low T_g peak moves closer to the pure PBzA transition (2 °C), indicating that the soft phase has



become more PBzA rich and that there is less blending of the two phases. McAllister et al.³² observed similar trends in DMA data for the alternative two-monomer system (PMMA/PDMAEMA) that produced an internal core-shell like morphology.

To probe the structure and internal morphology of the PMMA/PBzA particles further, scanning electron microscopy (SEM) and transmission electron microscopy (TEM) coupled with preferential staining were used. Preferential staining is a common technique used to distinguish the internal morphology of two component particles.⁴⁹ SEM analysis showed that the particle structure was well maintained as the BzA loading increased, with uniform, monodisperse particles being formed (Figure 5)

In TEM analysis, the presence of the phenyl ring in the PBzA allows for preferential staining of this phase with RuO₄.⁵⁰ Pure PMMA particles appeared homogeneous and no visible internal morphology was observed. A dark ring was observed on the surface of the particle, which is attributed to the PDMS-MA stabiliser (Figure 5).³² DMA analysis also implies that only one of the phases is present. The particles obtained using a feed of 9 wt% BzA also appear homogeneous with no visible morphology observed in the TEM image (Figure 5). This again agrees with GPC and DMA analysis. The presence of two distinct, separate phases was faintly visible in particles synthesised with a BzA loading of 27 wt% showing a PMMA core encased in a PBzA shell (Figure 5).

As the BzA loading was increased further to 36 wt%, the internal morphology begins to change, showing smaller internal domains of PBzA surrounded by a continuous PMMA phase (Figure 5). A possible explanation is that under the conditions used (207 bar and 65 °C), the PMMA seed particles will be plasticised,¹¹ allowing for facile penetration of a second monomer/polymer.³² For the particles synthesised with a loading of 50 wt%, it also appears



that the PBzA is apparently has migrated into the PMMA particles. Phase separation in particles synthesised using emulsion polymerisation is a well-studied area and the internal morphology formed is influenced by a combination of thermodynamic and kinetic factors.^{24,25} Particles produced under thermodynamic control will lead to a morphology that is at equilibrium and is driven by a minimisation of the interfacial free energy. However, in most cases the internal morphology formed is controlled by kinetics. Three kinetic factors control the morphology; (1) radical penetration into the seed particles during the second stage of the polymerisation, (2) polymer phase-separation and (3) consolidation of the phase domains after phase separation.^{24,25,51} In our system, increasing the PBzA concentration certainly has an effect on the morphology and it could be that the higher concentration is enhancing kinetic factors and aiding phase separation.

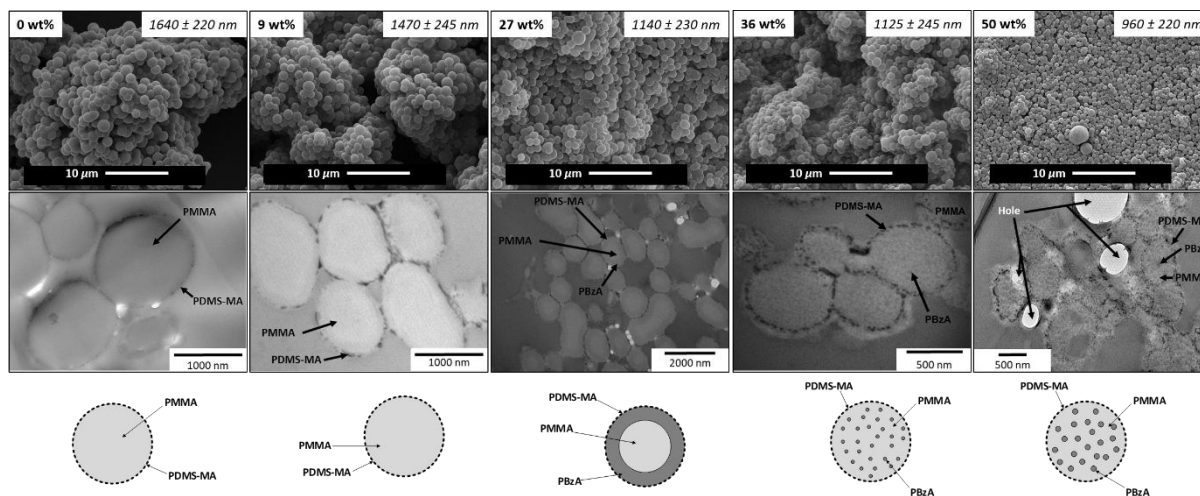


Figure 5: Images showing SEM (top) and TEM (middle) for pure PMMA particles (left) and particles synthesised using feeds of 9, 27, 36 and 50 wt% (left to right) of BzA. Particle size with standard deviation is given. A schematic representation (bottom) shows the internal morphology present. A loading of 27 wt% exhibited an inverse core-shell morphology. The two loadings above 27 wt% exhibited the presence of small internal domains of PBzA surrounded by PMMA.

Another factor that could be influencing the observed morphologies is molecular weight. As the loading of BzA is increased, the molecular weight of the PBzA phase formed also increased



(indicated by a shift to lower retention time in the GPC trace (Figure 3)). This change in

View Article Online
DOI: 10.1039/D0PY00729C

molecular weight could induce the formation of a different morphology, as has previously been reported for block copolymers.^{20,24,52} CO₂-philicity of the monomer and its corresponding polymer could also be an influencing factor on the morphology produced.^{20,29,32} For example, a more CO₂-phobic monomer/polymer would prefer to migrate inside the PMMA particle and thus limit its interaction with CO₂. In addition, the variation in particle size of the seed PMMA could also be altering the morphology produced.^{24,53}

Further work is ongoing to understand the driving force for the morphology formed. However, this may be a promising new method to synthesise particles with complex morphologies, which does not require the use of controlled polymerisation techniques to produce block copolymers.

Particles containing phase-separated hard and soft domains have been successfully synthesised, to produce a core-shell structure as well as a micro-phase separated structure consisting of soft spheres in a hard matrix. Partial blending of the PMMA with the PBzA phase increased the T_g of the soft domains to above room temperature. Thus, a lower T_g soft block was also investigated to ensure the presence of a soft phase at room temperature.

Poly(butyl acrylate) (PBA) was chosen as an alternative, more industrially relevant soft polymer (T_g: -45 °C). PBA is traditionally used for a wide range of applications such as impact modification.⁵⁴⁻⁵⁸ The same two-stage method was used, in which PMMA seed particles were synthesised before the addition of BA. Various loadings of BA were tested (Table 4).



Table 4: Summary of two-stage reactions carried out with various loadings of BA. All reactions were completed in duplicate to check batch-to-batch variability.

Entry	BA Target Loading (wt%)	PBA Content ^a (wt%)	BA Conversion ^a (%)	BA Loading by NMR ^{a*} (wt%)	Particle Size ^b (nm)
1	0	0	0	0	1640 ± 220
2	9	5	71	7	1700 ± 220
3	27	21	68	28	900 ± 150

^a - calculated from ¹H NMR, ^b - measured from SEM images (including standard deviation), *calculated post reaction from unreacted BA and PBA content.

BA conversion was calculated from ¹H NMR by comparison of the unreacted monomer signal (Figure 6, $\delta = 6.12$ ppm, d) to polymer signal (Figure 6, $\delta = 4.04$ ppm, d'). Just like the BzA system, the presence of unreacted BA (Figure 6, $\delta = a, b$ and c) could affect the T_g of the material. As the quantity of unreacted monomer was found to be relatively high, the samples were flushed with CO₂ post polymerisation for 15 minutes at room temperature to ensure removal of BA monomer prior to DMA analysis.

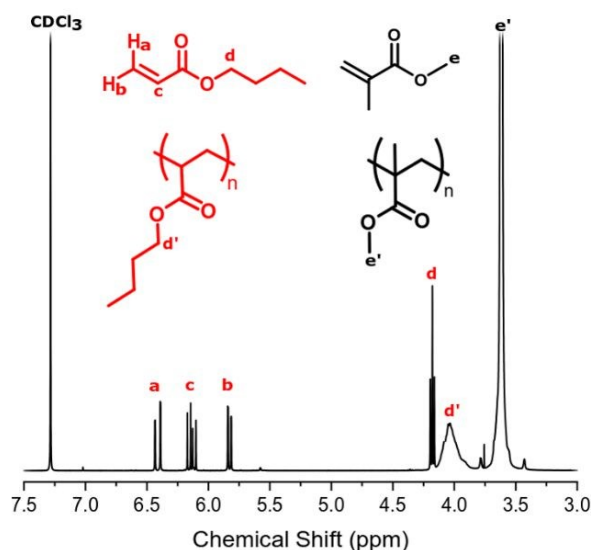


Figure 6: ¹H NMR trace for a reaction containing PBA run in chloroform. Integration values were used to calculate conversion and content of the second monomer. The reaction was carried out using a BA loading of 27 wt%, employing the two-stage experimental method.



PBA content was calculated by comparison of the PMMA signal (Figure 6, $\delta = 3.60$ ppm, e) to the PBA signal (Figure 6, $\delta = 4.04$ ppm, d'). At both loadings, BA conversion reached <75% and increasing the reaction time did not lead to any further increase. The reasons for this lower conversion when compared to the BzA system are unclear and further investigation is needed. The PBA content of the particles was slightly lower than the feed for both loadings, which reflects the BA conversion of <75%. However, as the feed loading is increased, an increase in PBA content was observed. The loading of BA measured by ^1H NMR post reaction (unreacted monomer + polymer) was similar to the target loading, indicating that the desired loading of BA was achieved (Table 4).

In GPC analysis, the DRI trace for a BA loading of 9 wt% showed a unimodal peak. By contrast, multimodal peaks were observed for the higher loading of 27 wt% (Figure 7). The UV comparison carried out for PBzA containing particles could not be done here as PBA is not UV active.

The DMA trace for pure PMMA shows two clear peaks (Figure 7, black traces) at 144 °C, corresponding to the T_g of the PMMA phase; and at -50 °C, corresponding to the melting transition (T_m) of the stabiliser used (PDMS-MA). A small amount of this PDMS-MA is known to be incorporated into the particles via the stabilisation mechanism of the dispersion polymerisation.⁴⁴ Concentrating on the "PMMA type" peak, the addition of 9 wt% of BA caused a shift to a lower temperature suggesting that the phases present are not completely separated but partially blended (Figure 7).⁵⁹ The peak is also broad in comparison to the PMMA particles, with what could be considered as a small lower temperature shoulder peak. This suggests that there is a large variation in composition, with lower T_g s being measured for the material in the sample containing a higher amount of PBA. As the BA loading was increased to 27 wt%, the "PMMA type" peak becomes less well-defined. The peak also shifts



to a lower temperature and broadens further, with the shoulder peak becoming slightly more defined.

Focusing on the low temperature region, three peaks are visible. As previously discussed, if a core-shell morphology was present, then a T_g peak for both the “soft” PBA phase and the “hard” PMMA phase of the particles would be observed. Although one of these peaks occurs in a similar position to PBA homopolymer, in this system, the crystal melt of the PDMS-MA stabiliser, occurs at $-50\text{ }^\circ\text{C}$, which is very close to the expected T_g of PBA at $-45\text{ }^\circ\text{C}$ (Figure SI-4 in the SI).

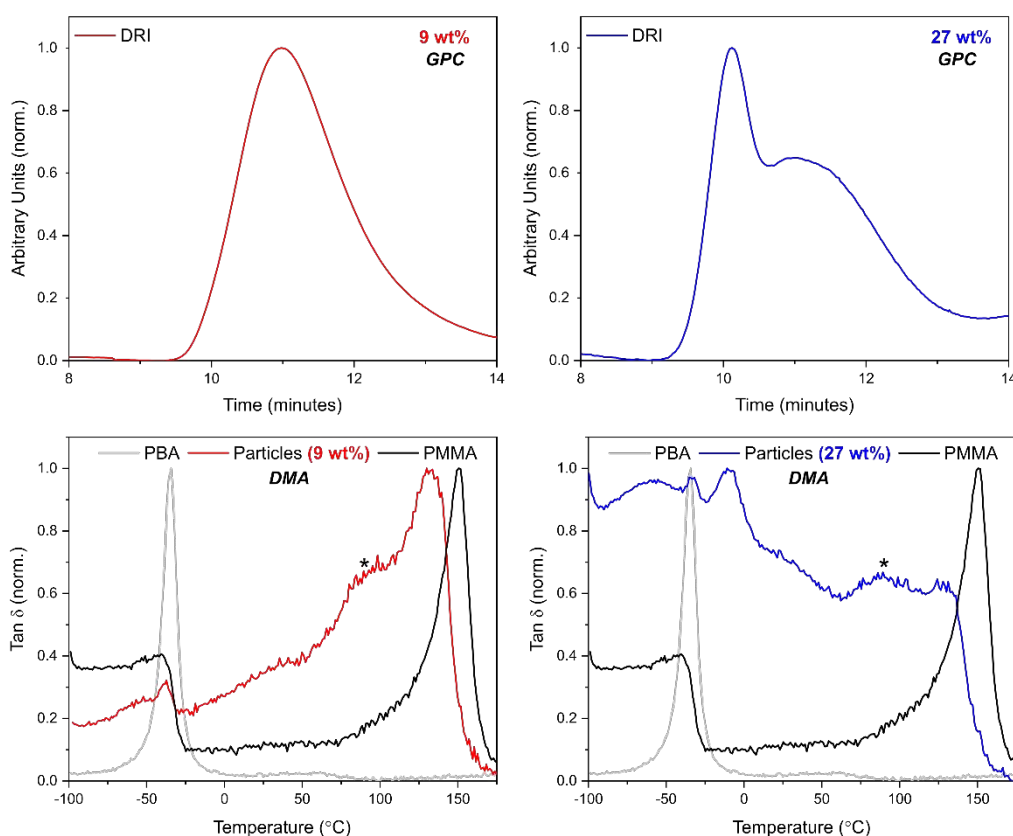


Figure 7: GPC (top) and DMA (bottom) for particles synthesised used 9 wt% (red) and 27 wt% (blue) BzA. GPC analysis indicated one species is present at 9 wt% loading, whereas two are present for 27 wt%. A DMA trace for homopolymer of PBzA (grey) and PMMA particles (black) is given for comparison. Both loadings showed the presence of a PMMA rich phase but overlap of the PBA and PDMS-MA transition made it difficult to decipher if full phase separation had occurred. Shoulder peaks are highlighted by a *. Samples were extracted with scCO_2 to remove unreacted monomer prior to DMA analysis.



It is therefore very difficult to determine if a homogeneous PBA peak was present using thermal analysis. For the 27 wt% loading, a peak at -8 °C was observed suggesting the presence of a PBA rich phase (Figure 7). This peak is at a higher temperature than the PBA homopolymer (-45 °C), which indicates that blending of PMMA with this phase may be occurring.

SEM analysis showed that particle structure was maintained as the BA loading was increased (Figure SI-5). However, due to the similarities in functional groups between the two monomers used (MMA and BA), the use of TEM analysis coupled with preferential staining of one phase was not possible. In the absence of TEM analysis, atomic force microscopy (AFM) analysis can be used to gain an insight into the surface structure of particles.^{60,61} Measurements performed in PF-QNM mode can provide synchronized information about surface mechanical properties, including localised modulus and adhesion. Although, used in this way, this technique cannot give any information about the internal structure. AFM was used to probe to surface of the particles containing PBA (27 wt%) (Figure 8).

Initial AFM imaging of the PMMA/PBA particles clearly show that a network-like structure is present on the surface for PMMA/PBA (27 wt%) (Figure 8). By contrast, for the particles made up of just PMMA the surfaces of the particles are featureless. Further work must be performed to definitively show that full phase separation has occurred, and to determine which of the components of the components in the PMMA/PBA (27 wt%) corresponds to each polymer.

Our observations suggest that the changes in the low temperature region of the DMA trace, notably the appearance of a peak at -8 °C, indicates the presence of a PBA rich phase which is also supported by the observation of extra peaks in the GPC chromatogram. From the AFM data coupled with the other analytical techniques, it was concluded that a PMMA and a PBA



phase were likely to be present and it was possible that the system had formed a particle with

a low T_g shell and high T_g core.

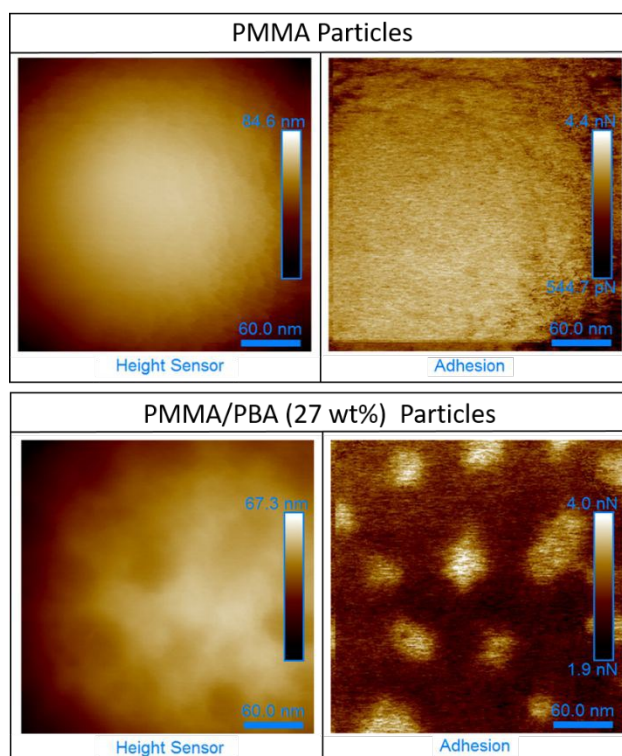


Figure 8: AFM images recorded of PMMA particles (top) and particles synthesised with a feed of BA (27 wt%) (bottom). A network of PBA is present on the surface of the particle synthesised with BA is observed, as indicated by the arrows. The scale bar in all images is 60 nm.

Conclusions

Successful addition of either BA or BzA (low T_g), at various loadings, to preformed PMMA particles was demonstrated. The two-stage reaction technique utilising $scCO_2$ as the reaction medium was used to synthesise PMMA particles containing a feed of up to 36 wt% BzA. For a loading of 50 wt%, the addition of BzA was split over two charges in order to maintain particle quality. SEM analysis showed that particle structure did not deteriorate significantly as the loading of BzA was increased up to 50 wt%. DMA analysis indicated two separate T_g s, signifying the presence of two phases. This was complemented by GPC analysis, which also suggested the presence of two different species: PMMA and PBzA chains of different



molecular weights, confirmed by UV analysis. Furthermore, TEM analysis showed the presence of internal morphology; at 27 wt% a PMMA core encased in a PBzA shell was formed and at both 36 and 50 wt%, small internal domains of PBzA surrounded by a continuous PMMA phase was observed. This suggests that the morphology formed is dependent on the concentration of PBzA but may be related to other factors such as particle size and molecular weight.

Moving to a more industrially relevant system, an alternative soft polymer component of PBA was tested. Once again, the SEM analysis indicated that the structure of the particles did not deteriorate as the PBA content increased. At low loadings of BA, DMA suggested that the particles produced were homogeneous, containing one phase as opposed to the desired core-shell structure, containing two phases. Nevertheless, as the BA loading was increased, the DMA analysis suggested the presence of a PBA rich phase, but it is difficult to say for certain because the T_g of the PBA phase and the PDMS-MA occur at very similar temperatures. AFM analysis showed the formation of a network-like structure of on the surface of the particles. The work presented is a simple and novel method to synthesis phase-separated particles in $scCO_2$ that does not require any chemical control agents or post-polymerisation drying steps. Further work and adjustments are needed to enable full control and understanding of the internal morphology produced for each monomer at the various loadings.

Acknowledgements

The authors thank M. C. Dellar, P. Fields, R. Wilson, M Guyler, D. Litchfield and J. Warren for their technical and engineering input. The authors also gratefully acknowledge the University of Nottingham Nanoscale and Microscale Research Centre (nmRC) for access to their

instrumentation, in particular Denise Mclean and Nicola Weston for help with the TEM analysis.

View Article Online
DOI: 10.1039/C9PY00729C

References

1. M. d. A. Gamiero, A. R. Goddard, V. Taresco and S. M. Howdle, *Green Chemistry*, 2020.
2. J. L. Kendall, D. A. Canelas, J. L. Young and J. M. DeSimone, *Chemical Reviews*, 1999, **99**, 543-564.
3. A. I. Cooper, *Journal of Materials Chemistry*, 2000, **10**, 207-234.
4. J. M. DeSimone, Z. Guan and C. S. Elsbernd, *Science*, 1992, **257**, 945-947.
5. D. A. Canelas and J. M. DeSimone, *Metal Complex Catalysts Supercritical Fluid Polymerization Supramolecular Architecture*, 1997, **133**, 103-140.
6. M. R. Clark and J. M. DeSimone, *Macromolecules*, 1995, **28**, 3002-3004.
7. M. R. Clark, J. L. Kendall and J. M. DeSimone, *Macromolecules*, 1997, **30**, 6011-6014.
8. S. Curia and S. M. Howdle, *Polymer Chemistry*, 2016, **7**, 2130-2142.
9. D. D. Hile and M. V. Pishko, *Macromolecular Rapid Communications*, 1999, **20**, 511-514.
10. D. D. Hile and M. V. Pishko, *Journal of Polymer Science Part A: Polymer Chemistry*, 2001, **39**, 562-570.
11. J. M. DeSimone, E. E. Maury, Y. Z. Menciloglu, J. B. McClain, T. J. Romack and J. R. Combes, *Science*, 1994, **265**, 356-359.
12. A. M. Gregory, K. J. Thurecht and S. M. Howdle, *Macromolecules*, 2008, **41**, 1215-1222.
13. G. Hawkins, P. B. Zetterlund and F. Aldabbagh, *Journal of Polymer Science Part A: Polymer Chemistry*, 2015.
14. K. J. Thurecht and S. M. Howdle, *Australian Journal of Chemistry*, 2009, **62**, 786-789.
15. J. Xia, T. Johnson, S. G. Gaynor, K. Matyjaszewski and J. M. DeSimone, *Macromolecules*, 1999, **32**, 4802-4805.
16. P. B. Zetterlund, F. Aldabbagh and M. Okubo, *Journal of Polymer Science Part A: Polymer Chemistry*, 2009, **47**, 3711-3728.
17. A. I. Cooper, W. P. Hems and A. B. Holmes, *Macromolecular Rapid Communications*, 1998, **19**, 353-357.



18. T. Hasell, K. J. Thurecht, R. D. W. Jones, P. D. Brown and S. M. Howdle, *Chemical Communications*, 2007, 3933-3935. View Article Online
DOI: 10.1039/B6PY00729C
19. J. Jennings, M. Beija, J. T. Kennon, H. Willcock, R. K. O'Reilly, S. Rimmer and S. M. Howdle, *Macromolecules*, 2013, **46**, 6843-6851.
20. J. Jennings, M. Beija, A. P. Richez, S. D. Cooper, P. E. Mignot, K. J. Thurecht, K. S. Jack and S. M. Howdle, *Journal of the American Chemical Society*, 2012, **134**, 4772-4781.
21. J. Jennings, G. He, S. M. Howdle and P. B. Zetterlund, *Chemical Society Reviews*, 2016, **45**, 5055-5084.
22. A. Aguiar, S. González-Villegas, M. Rabelero, E. Mendizábal, J. E. Puig, J. M. Dominguez and I. Katime, *Macromolecules*, 1999, **32**, 6767-6771.
23. S. Kawaguchi and K. Ito, in *Polymer Particles*, Springer, 2005, pp. 299-328.
24. D. C. Sundberg and Y. G. Durant, *Polymer Reaction Engineering*, 2003, **11**, 379-432.
25. J. M. Stubbs and D. C. Sundberg, *Progress in Organic Coatings*, 2008, **61**, 156-165.
26. S. M. Thaker, P. A. Mahanwar, V. V. Patil and B. N. Thorat, *Drying Technology*, 2010, **28**, 669-676.
27. T. D. McAllister, L. D. Farrand and S. M. Howdle, *Macromolecular Chemistry and Physics*, 2016, **217**, 2294-2301.
28. S. P. Bassett, A. D. Russell, P. McKeown, I. Robinson, T. R. Forder, V. Taresco, M. G. Davidson and S. M. Howdle, *Green Chemistry*, 2020.
29. J. Jennings, S. P. Bassett, D. Hermida-Merino, G. Portale, W. Bras, L. Knight, J. J. Titman, T. Higuchi, H. Jinnai and S. M. Howdle, *Polymer Chemistry*, 2016, **7**, 905-916.
30. L. Cao, L. Chen, X. Chen, L. Zuo and Z. Li, *Polymer*, 2006, **47**, 4588-4595.
31. C. F. Lee, M. L. Hsu, C. H. Chu and T. Y. Wu, *Journal of Polymer Science Part A: Polymer Chemistry*, 2014, **52**, 3441-3451.
32. T. D. McAllister, T. M. Bennett, C. Petrillo, C. Topping, L. Farrand, N. Smith and S. M. Howdle, *Journal of Materials Chemistry C*, 2019, **7**, 12194-12203.
33. J. Liu, X. Tian, J. Sun and Y. Yuan, *Journal of Applied Polymer Science*, 2016.
34. H. Teng, K. Koike, D. Zhou, Z. Satoh, Y. Koike and Y. Okamoto, *Journal of Polymer Science Part A: Polymer Chemistry*, 2009, **47**, 315-317.
35. J. Brandrup, E. H. Immergut, E. A. Grulke, A. Abe and D. R. Bloch, *Polymer handbook*, Wiley New York, 1999.
36. G. Heal, *Principles of thermal analysis and calorimetry*, 2002, **52**.



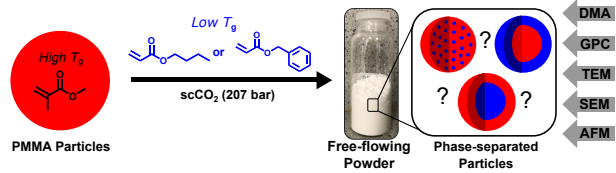
37. G. F. Wu, J. F. Zhao, H. T. Shi and H. X. Zhang, *European Polymer Journal*, 2004, **40**, 2451-2456. View Article Online
DOI: 10.1059/E040729C
38. Q. B. Si, C. Zhou, H. D. Yang and H. X. Zhang, *European Polymer Journal*, 2007, **43**, 3060-3067.
39. P. Christian, S. M. Howdle and D. J. Irvine, *Macromolecules*, 2000, **33**, 237-239.
40. A. J. Haddleton, S. P. Bassett and S. M. Howdle, *The Journal of Supercritical Fluids*, 2020, **160**, 104785.
41. Z. Guan, J. R. Combes, Y. Z. Menciloglu and J. M. DeSimone, *Macromolecules*, 1993, **26**, 2663-2669.
42. M. R. Giles, J. N. Hay and S. M. Howdle, *Macromolecular Rapid Communications*, 2000, **21**, 1019-1023.
43. W. Wang, M. R. Giles, D. Bratton, D. J. Irvine, S. P. Armes, J. V. W. Weaver and S. M. Howdle, *Polymer*, 2003, **44**, 3803-3809.
44. M. R. Giles, J. N. Hay, S. M. Howdle and R. J. Winder, *Polymer*, 2000, **41**, 6715-6721.
45. T. M. Bennett, G. He, R. R. Larder, M. G. Fischer, G. A. Rance, M. W. Fay, A. K. Pearce, C. D. Parmenter, U. Steiner and S. M. Howdle, *Nano Letters*, 2018, **18**, 7560-7569.
46. K. P. Lok and C. K. Ober, *Canadian Journal of Chemistry*, 1985, **63**, 209-216.
47. N. M. Ahmad, F. Heatley and P. A. Lovell, *Macromolecules*, 1998, **31**, 2822-2827.
48. M. Chen, C. Zhou, Z. Liu, C. Cao, Z. Liu, H. Yang and H. Zhang, *Polymer International*, 2010, **59**, 980-985.
49. M. Gosecka and M. Gosecki, *Colloid and Polymer Science*, 2015, **293**, 2719-2740.
50. J. S. Trent, J. I. Scheinbeim and P. R. Couchman, *Macromolecules*, 1983, **16**, 589-598.
51. M. Okubo, J. Izumi, T. Hosotani and T. Yamashita, *Colloid and Polymer Science*, 1997, **275**, 797-801.
52. B. Sarkar and P. Alexandridis, *Progress in Polymer Science*, 2015, **40**, 33-62.
53. S. Li, P. Chen, L. Zhang and H. Liang, *Langmuir*, 2011, **27**, 5081-5089.
54. L. J. Borthakur, T. Jana and S. K. Dolui, *Journal of coatings technology and research*, 2010, **7**, 765-772.
55. A. K. Khan, B. C. Ray, J. Maiti and S. K. Dolui, *Pigment & Resin Technology*, 2009.
56. W. Li, Y. Zhang, D. Wu, Z. Li, H. Zhang, L. Dong, S. Sun, Y. Deng and H. Zhang, *Advances in Polymer Technology*, 2015.



57. W.-G. Yao, L.-Q. Wang, D.-Y. He, S.-C. Jiang, L.-J. An and H.-X. Zhang, *Chinese Journal of Polymer Science*, 2005, **23**, 337-340.
58. W. Ye, M. F. Leung, J. Xin, T. L. Kwong, D. K. L. Lee and P. Li, *Polymer*, 2005, **46**, 10538-10543.
59. A. I. Isayev, *Encyclopedia of Polymer Blends, Volume 3: Structure*, John Wiley & Sons, 2016.
60. S. H. Kim, W. K. Son, Y. J. Kim, E. G. Kang, D. W. Kim, C. W. Park, W. G. Kim and H. J. Kim, *Journal of Applied Polymer Science*, 2003, **88**, 595-601.
61. F. Sommer, T. M. Duc, R. Pirri, G. Meunier and C. Quet, *Langmuir*, 1995, **11**, 440-448.

View Article Online
DOI: 10.1039/C5PY00729C





View Article Online
DOI: 10.1039/D0PY00729C

